Investigation of a Complex Mountain Wave Situation

RALPH D. REYNOLDS AND ROY L. LAMBERTH

Atmospheric Sciences Office, White Sands Missile Range, N. Mex.

AND M. G. WURTELE

University of California at Los Angeles

(Manuscript received 27 February 1968)

ABSTRACT

A complex mountain lee wave was recorded by radar-tracked superpressure balloons at White Sands Missile Range on 6 May 1965 at a mean altitude of 3.5 km MSL; simultaneously, a very weak wave was recorded at 7 km. The lower complex wave showed variable wavelengths, amplitudes, and increasing vertical velocities with time.

Several of the better existing mountain wave theories were tested against the data to determine which theory or theories, if any, could explain the physical cause of the particular features of the complex wave.

It was found that existing theoretical models are too simplified to apply to the condition in the observed wave and explain only its grosser features. If our understanding of gravity waves is to be adequate to explain quantitatively what we are capable of observing quantitatively, we must begin the anlysis of more realistic models or turn to numerical integration of the relevant equations.

1. Introduction

The basic mission of the mountain wave study at White Sands Missile Range (WSMR) is to furnish the ballistic meteorologist with a workable method for determining the occurrence, location, and strength of lee waves over the missile range.

The WSMR mountain wave study has been in operation for five spring seasons and over 200 radar plots of balloon flights have been obtained. Of these radar plots, 30% showed no detectable wave, 50% showed a simple wave pattern, and 20% showed a complex wave pattern. A "complex wave pattern" is defined here as a series of waves in horizontal succession displaying variable wavelengths and amplitudes. Of these complex waves only the one that showed a well-defined wave system both upwind of the San Andres Mountains and also downstream over the missile range was investigated in depth. This complex wave shows alterations in its wavelength

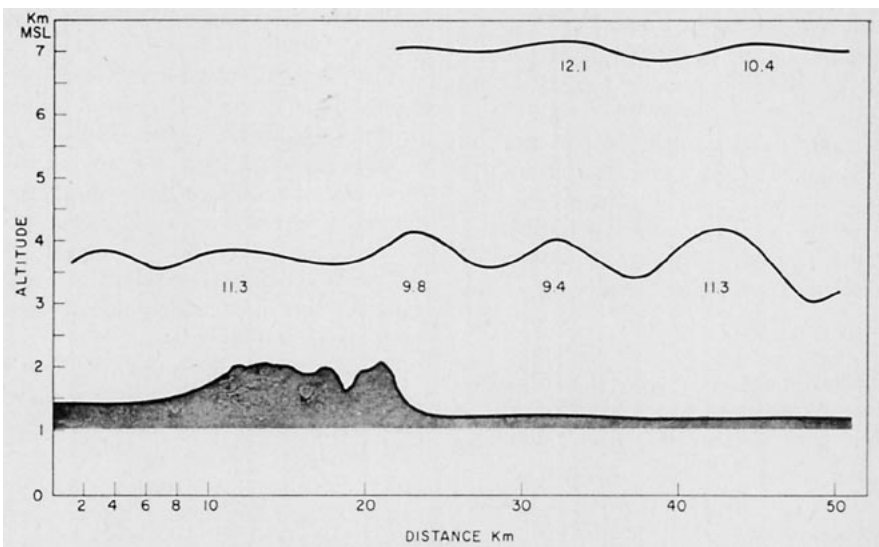

FIG. 1. The cross section of two waves recorded on 6 May 1965 with the complex wave being at a mean altitude of 3.5 km. The wavelength of each wave is shown. The first wavelength in the complex series is incomplete, the following waves being measured from trough-to-trough positions. The upper wave at 7 km displays a very small amplitude.

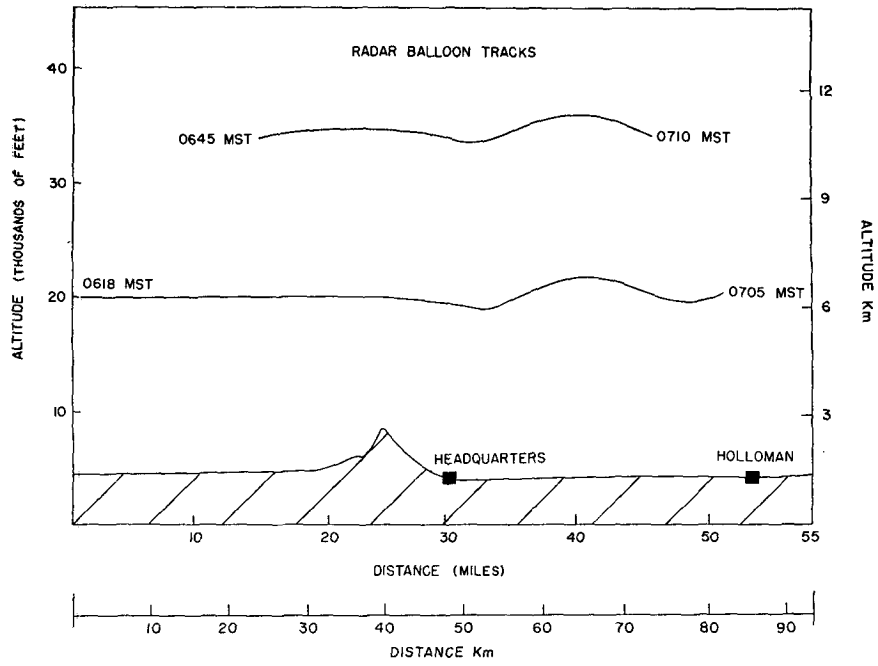

FIG. 2. Balloon tracks for 1 April 1964 showing the straight, level flow of a balloon prior to reaching the mountains. This straight line flow is characteristic of mountain wave balloon tracks prior to reaching the mountains.

and amplitude with time, and the vertical velocity increased from 2.8 to 5.0 m sec^{-1}.

Most of the mountain wave theories give an adequate answer for the location and intensity of a wave of simple sinusoidal type damping with time, but none of the theories apply to complex waves *per se*. Since 20% of the recorded waves at WSMR are complex, it was decided to test applicable lee-wave theories against this particular complex wave to determine which theory or theories, if any, could explain its observed features.

One hypothesis that may be suggested by inspection of the complex wave (the lower wave in Fig. 1) is that there is a superposition on a residual upstream wave, initiated by the mountain and resulting in resonance or reinforcement in the downstream waves. Accepting this hypothesis, we ask which of the current theories are applicable to this particular situation, and which theory or theories may be used by the ballistic meteorologist to forecast the location and strength of complex lee waves.

2. Background

A mountain lee wave is a gravity wave that is caused by, and is stationary with respect to, some barrier in the fluid flow. The time scale of buoyancy has a characteristic frequency, the Brunt-Väisaala frequency, $\omega=[(g/\theta)(\partial\theta/\partial z)]^{\frac{1}{2}}$, where g is the acceleration of gravity and θ is potential temperature.

The linearized mountain wave equation may be expressed in the form

$$\partial^2 w/\partial z^2+(L^2-k^2)w=0, \qquad (1)$$

where

$L^2=\omega^2/U^2-\partial^2 U/\partial z^2$,
w = vertical velocity,
k = horizontal wavenumber,
U = horizontal wind speed in the undisturbed flow,
z = height.

The mountain wave theory indicates that the wavelength of any lee waves will lie between the maximum and minimum values of $2\pi/L$ through the troposphere (Alaka, 1960).

The mountain wave study field test precedures, using especially adapted AMT/15 radiosondes flown on superpressure balloons, have been reported previously (Lamberth *et al.*, 1965; Reynolds and Lamberth, 1966). However, it should be pointed out that the balloon-detected wave cross sections shown in the illustrations were taken from the computer reductions of the AN/FPS-16 radar digital data, recorded on magnetic tape at a rate of one data point per second and smoothed over 30-sec intervals.

Booker and Cooper (1965) have shown that superpressure balloons tend to follow the free airstream with good fidelity while traversing mountain waves; so it is believed that the true airstream flow during these reported mountain wave conditions is accurately depicted by the radar-tracked oscillations of the superpressure balloons.

3. The complex wave and its associated parameters

One of the more unusual aspects of the complex wave of Fig. 1 is the existence of a fairly well defined gravity

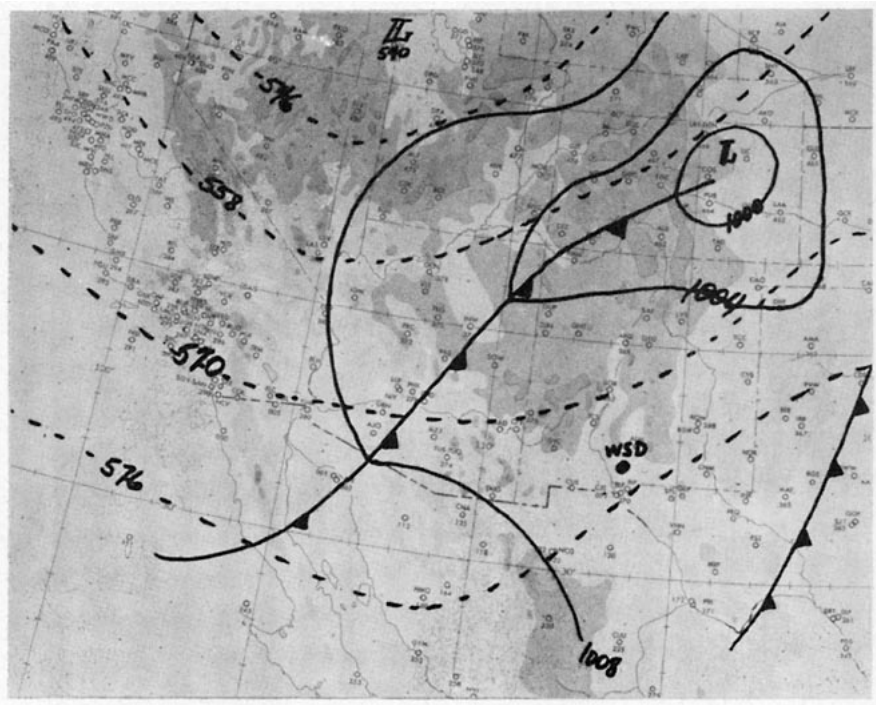

FIG. 3. 500-mb contours (dashed lines) showing a long-wave trough position centered over the Great Basin area. The surface cold front is approaching White Sands Missile Range (WSD) from the west.

wave upstream of the San Andres Mountains, caused most probably by mountains further west of WSMR. This is the only dominant pre-mountain wave that has been recorded during our mountain wave study—the recorded air flow upstream of the San Andres has always been smooth and level. The normal situation is shown in Fig. 2, in which the wave begins in the lee of the San Andres. (To simplify references hereafter to any portion of the complex wave, the waves will be referred to as wave A for the first wavelength through wave E for the

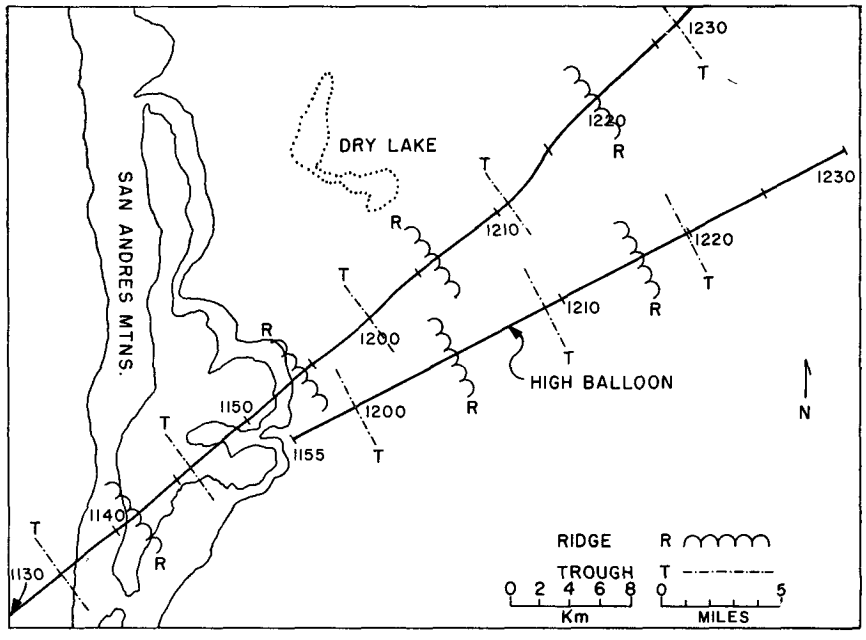

FIG. 4. Radar-balloon tracks for 6 May 1965 showing that the two balloons were close in time and space. The steepest escarpment of the San Andres lies to the west of the Dry Lake where San Andres Peak rises more than 4000 ft above the valley floor.

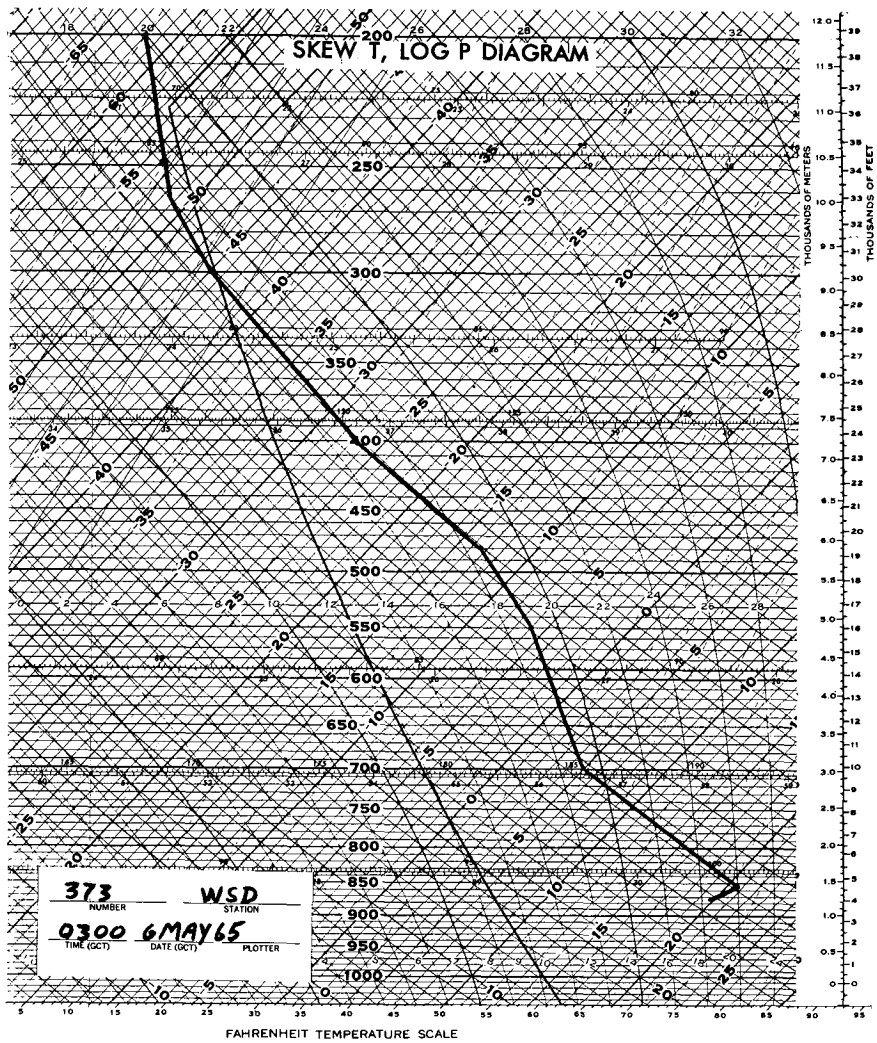

FIG. 5. Temperature profiles showing dry adiabatic lapse rates in the layer above the surface inversion and between 5.9 to 7.2 km. The lapse rate is moist adiabatic between 3.0 to 4.9 km. Each specific stability regime above the surface boundary layer was used in the calculation of L^2.

last wave.) As shown in Fig. 1, wave B with amplitude of 300 m in the complex series is exactly in phase with the first ridge of the mountain and wave C shows a definite increase in amplitude to 580 m; this suggests that resonance or reinforcement might be present. Wave D has an amplitude of 580 m, which increases in E to 1165 m. This increase did not follow through to the upper levels where it is seen that the waves at 7 km are very weak, with wavelengths of 10 and 12 km.

The vertical velocities ranged from a maximum of 1.0 m sec^{-1} in waves A and B to 2.9 m sec^{-1} in waves C and D to a maximum of 5.0 m sec^{-1} near the last inflection point of wave E.

Prior to and during the recording of the complex mountain wave, the sky was cloudless. The relative humidity went below the threshold of measurement. A long-wave trough was centered over Utah and western Arizona. A minor trough accompanied the cold front moving through central Arizona to Colorado (Fig. 3).

The west-east cross section is shown in Fig. 1 for the mountain wave and the mountain; the mountain range is orientated basically north-south. The wavelengths shown are for the u component of the waves. The horizontal trajectories of the two balloons are plotted in Fig. 4 where it may be seen that the balloons were close in time and space.

A rawinsonde was released at 0300 MST, 12.8 km south of the 1200 MST position of the balloon track shown in Fig. 4. The temperature from this rawinsonde is shown in Fig. 5 plotted on a skew T, log p diagram. There are seven discernible changes in the lapse rate and/or velocity profile from the surface to 200 mb. A second rawinsonde was released from the same position as the 0900 MST release at 0900 MST. The only difference in

the two observations was that a superadiabatic lapse rate existed near the surface at 0900 MST.

The normal wind profile, which in this case is also a zonal wind profile, is shown in Fig. 6, calculated from the 0300 MST rawinsonde.

The L^2 profile was computed noting the near-adiabatic layers from 1.5–3 km and from 6–7 km. Values for L^2 were determined at the 3-, 6-, 7.2-, 9.2- and 11-km levels, these being chosen such that a linear variation between consecutive points gave a good approximation. This profile up to 11 km has been plotted in Fig. 7.

4. Quantitative application of theories

Analytical models exist for constant L^2 (Queney, 1947), for discontinuous layers of constant L^2 (Scorer, 1949), for exponentially decreasing L^2 (Palm and Foldvik, 1960), and for L^2 decreasing in the troposphere and constant in the stratosphere (Wurtele, 1953). However, the profile of L^2 in Fig. 7 as derived from real data is not easy to represent satisfactorily by any of these models.

The observed wave pattern shows the increasing wavelength and decreasing amplitude with height characteristic of decreasing L^2, rather than the up-wind tilt characteristic of constant L^2. So no attempt is made to apply the latter model. However, since the waves in question are observed at the 3.5-km level, it seems reasonable to attempt to explain the dynamics of the waves by the stable layer from 3–6 km, between the two neutral layers. To *this* segment of the profile, one may apply the Palm-Foldvik model with reasonable accuracy.

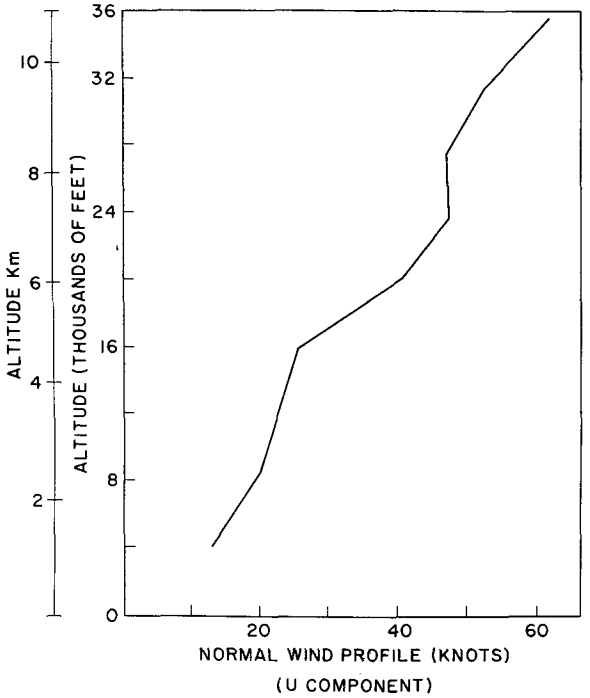

FIG. 6. The normal wind profile for 6 May 1965 showing an almost linear increase with height. This is also a zonal wind profile since the mountain range is orientated N-S.

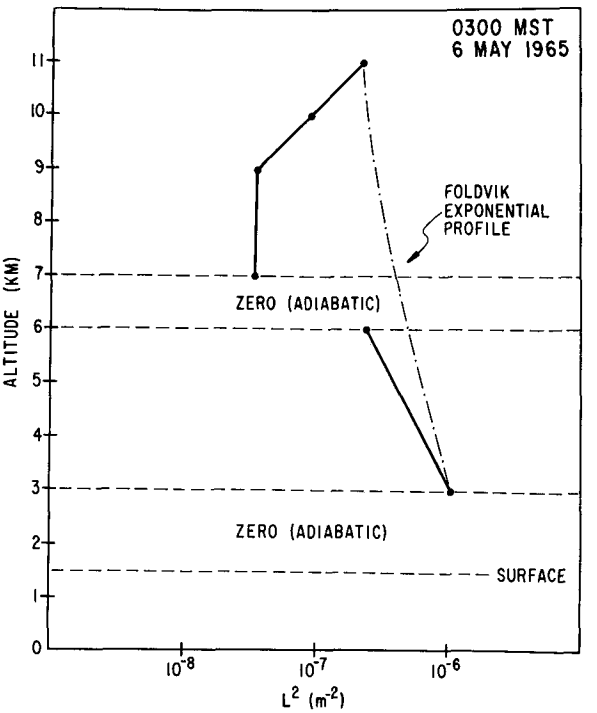

FIG. 7. The L^2 profile based on the 0300 MST rawinsonde. The dashed line represents the exponential curve fit to the two extreme points.

Let

$$L^2(z) = L^2(z_0)e^{-c(z-z_0)},$$

where the constant c is to be determined from the data. If we take z_0 as 3 km, then $c = 0.20$ km^{-1} for the 3–6 km layer. The eigensolution of Eq. (2) in this case is

$$w \sim J_{k/c}\left[\frac{L(z)}{c}\right], \tag{3}$$

where J is the Bessel function of the first kind. Free waves exist if and only if

$$J_{k/c}\left[\frac{L(0)}{c}\right] = J_{5k}(5) = 0. \tag{4}$$

In this case, $L(0) = 1$ km^{-1}, so that $k/c = 1.9$, $k = 0.38$ (Jahnke and Emde, 1945, p. 152) and the wavelength is about 16 km. This is much larger than anything observed, and we conclude that a much deeper layer than the 3–6 km layer is involved in the dynamics.

If the exponential profile is fit to the values of L^2 at 3 and 11 km, a value of $c = 0.133$ is obtained. The free waves are then given by

$$J_{7.5k}(7.5) = 0. \tag{5}$$

This yields two waves, $k = 1.25$ and 3.9 corresponding to wavelengths of 37.6 and 12.0 km. The shorter of these waves is in reasonable agreement, but the model is

clearly not to be expected to provide the significant details of the wave pattern, as can be seen by comparing the observed L^2 profile in Fig. 7 with the profile (dashed line) from the exponential model.

A rough estimate of the maximum vertical velocity associated with the 12-km wavelength, which will predominate over the longer wave in the lower levels, may be obtained from Foldvik (1962), i.e.,

$$|w|_{\max}=2.5+\frac{0.7}{cL(z_1)}hcU_{(0)}\left[\frac{\rho(0)}{\rho(z_1)}\right]^{\frac{1}{2}}, \tag{6}$$

where h is the mountain height and

$$z_1=\frac{1}{c}\ln\left[\frac{L_0}{L_0-2.2c}\right] \tag{7}$$

is the height at which this maximum value of vertical velocity is attained. Here $h=0.91$ km and $z_1=2.6$ km (above the 3-km level); thus, the theory predicts a maximum value of 4 m sec^{-1} at an elevation of 5.6 km associated with a wavelength of 12 km.

The downstream intensification and increasing wavelength are equally difficult to explain. A given mountain shape will tend to excite certain waves to greater amplitudes than others. For example, the mountain profile

$$k(x)=\frac{hb^2}{b^2+x^2}, \tag{8}$$

where b is the "half-width" of the mountain, leads to the spectral representation for vertical velocity

$$hU_0bkc^{-bk}, \tag{9}$$

so that the maximum forcing is given to the wave for which $bk=1$, or

$$L=2\pi b. \tag{10}$$

For $L\sim10$ km, this requires a mountain less than 1.5 km in half-width, which is a very steep escarpment.

It should be noted that both theory (Foldvik and Wurtele, 1967) and observation (Holmboe and Klieforth, 1957) agree that it is not the shape of the barrier as a whole that determines the "half-width" and therefore the forced waves, but only the lee-slope region. The relevance of this fact to the present problem is that when the balloon underwent amplification of its vertical velocity, it was opposite the steepest part of the San Andres lee escarpment.

A possible explanation of the wave pattern may in fact lie in the effects of the rather pronounced variation of the topography in the direction normal to the wind flow. In fact, the balloon tracks were over the most complex portion of the topography of the San Andres mountains. But a proper discussion of such a hypothesis requires abandonment of the two-dimensional assumptions employed exclusively so far in this paper.

For applicable three-dimensional analyses we may refer to Scorer and Wilkinson (1956) and Wurtele (1957). Unfortunately, these models apply to isolated peaks, whereas the peaks of the San Andres are presumably close enough to influence each other. In any case, if we apply the formulas of Wurtele (1957), we see that we expect maximum vertical velocities in crescent-shaped patterns, concave downwind and centered about 5 km downwind of each peak. These patterns do not superimpose to give the observed intensification.

No theory exists for a flow oblique to a ridge of profile similar to the San Andres.

5. Conclusions

If our understanding of gravity waves is to be increased, detailed L^2 profiles and streamlines at multiple levels are necessary. For this, the superpressure balloon is an excellent sensor, provided that adequate tracking facilities are available.

It is to be expected that once such data are gathered the simple theoretical models will be inadequate to explain many of the effects observed. In the instance discussed, the L^2 profile, first decreasing then increasing with height, is not one for which a theory exists; the topography of the barrier also introduced three-dimensional effects not tractable according to existing theory.

Since the simple theoretical models have had much success in producing operationally applicable formulas, it seems probable that the analysis of somewhat more complex models might well be worth attempting.

REFERENCES

Alaka, M. A., 1960: The airflow over mountains. WMO Tech. Note No. 34 (WMO No. 98, TP. 43), World Meteorological Organization, Geneva, 135 pp.

Booker, D. Ray, and Lynn W. Cooper, 1965: Superpressure balloons for weather research. *J. Appl. Meteor.*, **4**, 122–129.

Foldvik, A., 1962: Two-dimensional mountain waves—A method for the rapid computation of lee wavelengths and vertical velocities. *Quart. J. Roy. Meteor. Soc.*, **88**, 271–285.

——, and M. G. Wurtele, 1967: The computation of the transient gravity wave. *Geophys. J.*, **14**, 161–185.

Holmboe, J., and Harold Klieforth, 1954: Sierra Wave Project—Final Report. Contract No. AF 19(122)-263.

Jahnke, E., and Fritz Emde, 1945: *Tables of Functions*. New York, Dover Publ., Inc., 304 pp.

Lamberth, Roy L., R. D. Reynolds and M. G. Wurtele, 1965: Mountain lee waves at White Sands Missile Range. *Bull. Amer. Meteor. Soc.*, **46**, 634–636.

Palm, E., and A. Foldvik, 1960: Contribution to the theory of two-dimensional mountain waves. *Geophys. Norv.*, **21**, No. 6, 1–30.

Queney, P., 1947: Theory of perturbations in stratified currents with application to airflow over mountain barriers. The University of Chicago Press, Misc. Rept., No. 23.

Reynolds, Ralph D., and Roy L. Lamberth, 1966: Ambient temperature measurements from radiosondes flown on constant-level balloons. *J. Appl. Meteor.*, **5**, 304–307.

Scorer, R. S., 1949: Theory of waves in the lee of mountains. *Quart. J. Roy. Meteor. Soc.*, **75**, 41–55.

——, and Mary Wilkinson, 1956: Waves in the lee of an isolated hill. *Quart. J. Roy. Meteor. Soc.*, **82**, 419–427.

Wurtele, M. G., 1953: Two new models in the study of lee waves. Univ. of California, Los Angeles, Sci. Rept. No. 4, Contract AF 19(122)-263.

——, 1957: The three-dimensional lee-wave. *Beitr. Phys. Atmos.*, **29**, 242–251.